Ultra High Energy Cosmic Ray Production via Jet–Obstacle Interactions in Extragalactic AGN Jets

Author: Pol Quingles Daví
Facultat de Física, Universitat de Barcelona, Diagonal 645, 08028 Barcelona, Spain.

Advisor: Valentí Bosch, vbosch@fqa.ub.edu

Abstract: Jets of active galactic nuclei are potential accelerators of ultra high-energy cosmic rays. Some objects may reside in the jet region for extended periods and contribute to cosmic ray acceleration, especially of heavy nuclei. We explored the role of jet-object interactions inside extragalactic jets in producing UHECRs. Our goal was to characterize the maximum energies of particles accelerated in these events, likely dominated by heavy nuclei, and assess whether such interactions could act as UHECR acceleration sites. We found that jet-object interactions can be sufficiently efficient accelerators, producing cosmic rays with energies up to 100 EeV. These interactions may significantly contribute to the cosmic ray population.
Keywords: galaxies: active – galaxies: nuclei – galaxies: jets – cosmic rays
SDGs: ODSs 4 i 7

I. INTRODUCTION

The energy spectrum of cosmic rays spans more than ten orders of magnitude, from energies in the GeV range up to $\sim 10^{20}$ eV. It is characterized by a smooth power law over 11 decades of energy, with several inflection points; in the UHE regime, the most relevant features are the *ankle*, a hardening at ≈ 4 EeV, and a flux cutoff or suppression at ≈ 40 EeV (e.g., [2]; [3]). While supernova remnants are believed to be the most likely sources of cosmic rays at lower energies (i.e., up to the *knee* at $\sim 3 \times 10^{15}$ eV), the origin of ultra-high-energy cosmic rays (UHECRs, $E \geq 10^{18}$ eV = 1 EeV) is much less well understood and remains an open question since their discovery by Linsley [5]. Linsley measured the energy spectrum above 1 EeV and even carried out an analysis of arrival directions using a sample of 97 events. Since then, decades of experimental and theoretical work have been devoted to understanding the phenomenology and physics of UHECRs, but despite these efforts, their sources remain unidentified, as does the physics of their acceleration. Although they are thought to have an extragalactic origin, the actual astrophysical sources have yet to be pinpointed. Tracing back from the arrival directions to the UHECR sources remains a challenge due to limited statistics at the highest energies, uncertain detailed composition, and particularly the blurring effect of intergalactic and galactic magnetic fields (which are poorly known). Possible candidate sources include active galactic nuclei (AGNs) and their relativistic jets, starburst galaxies (SBGs), and gamma-ray bursts, as well as accretion shocks around galaxy clusters.

AGNs with jets have long been considered promising sources of UHECRs. As some of the most powerful and persistent sources in the universe, they are theoretically capable of meeting the physical requirements (e.g., size, energy) imposed on UHECR sources [3]. An important requirement for jets to act as UHECR accelerators is that the magnetic power of the jet must be sufficient to both accelerate and confine UHE particles. This power requirement is significantly reduced if the UHE particles have substantially higher charge than H or He (e.g., [2]; [6]). Experimental results seem to indicate that UHECR nuclei are, on average, heavy (around CNO-group masses) at energies $\gtrsim 10$ EeV (e.g., [7]).

From an experimental perspective, significant progress has been made in UHECR research over the past decade thanks to the Pierre Auger Observatory (PAO) and the Telescope Array (TA) collaborations, which have been instrumental in measuring the UHECR spectrum, composition, and anisotropy (aspects that will not be explored in this work). Fits to experimental data suggest a composition that becomes progressively heavier with increasing energy above the ankle [2]. The general trend is a gradual change from nearly pure protons around ~ 3 EeV to a heavier composition at higher energies [3].

Although this topic will not be addressed in detail in this TFG, a brief but important comment regarding the origin of the observed UHECRs is warranted in order to justify the value of L_j discussed below. Since UHECRs lose energy during their propagation through inelastic collisions with photons of the cosmic microwave background (CMB), AGN sources must be relatively nearby (i.e., within a few hundred Mpc) in order to account for the highest-energy cosmic rays observed. In recent years, particular attention has been paid to nearby AGNs—especially interesting candidate sources—such as the radio galaxies Centaurus A, M87, and Fornax A, motivated by current experimental data on UHECR anisotropy (e.g., [3]; [2]) and theoretical considerations.

This TFG will focus on the relevance of AGNs, including a concise discussion of particle acceleration in the relativistic jets of AGNs. In particular, to better understand the role of object–jet interactions occurring within AGN jets in the production of UHECRs, we carry out an initial exploration of these events as potential sites of

UHECR acceleration.

In Section II, a summary of some fundamental aspects of UHECRs is provided, establishing the basic assumptions that will be used throughout the work. In Section III, the scenario employed to perform the UHECR acceleration calculations is introduced; protons and electrons are discussed in separate subsections. Finally, the conclusions are presented in Section IV.

We generally adopt CGS units although energies are often given in eV or EeV. Unless otherwise stated, we adopt the convention $A_x \equiv (A/10^x \text{ cgs})$.

II. UHECR FUNDAMENTALS

The Hillas energy and power requirement

We define UHECRs as charged particles (protons or nuclei) reaching an energy in excess of 10^{18} eV, although a successful UHECR source must be able to accelerate particles right up to ~ 100 EeV in order to explain the full energy range of UHECR data. The spectrum of UHECRs arriving at Earth as measured by PAO is shown in Fig. 1 on [2] or in Fig. 1 on [3].

The Larmor radius (or gyroradius) of such an ultra-relativistic particle with energy $E \approx pc$ (where p is momentum) is given by $r_g = E/(ZeB)$. This is the radius of gyration when undergoing circular rotation in a uniform magnetic field. Writing down the Larmor radius already gives us useful insights. Given in scaling relation form for characteristic UHECR energies, the Larmor radius is:

$$r_g \approx 1.1 \text{ kpc} \left(\frac{E}{10 \text{ EeV}}\right) \left(\frac{B}{10\mu\text{G}}\right)^{-1} Z^{-1}. \quad (1)$$

This gives a (very minimal) condition for UHECR sources because a source must be able to confine a particle before it can accelerate it.

The maximum characteristic energy associated with a particle acceleration process is the Hillas energy [1], given by:

$$E_H = 9.25 \text{ EeV} \left(\frac{B}{10 \ \mu\text{G}}\right) \left(\frac{R}{\text{kpc}}\right) Z\beta, \quad (2)$$

where Z is the particle charge, $\beta = v/c$ is the velocity of the accelerator in units of c, B is the magnetic field, and R is the characteristic size of the acceleration region. Later on, we will use j as a subscript for these variables, referring to the acceleration site of a jet.

The Hillas condition is not merely that the Larmor radius equals the size of the region, but rather that it must be larger by a factor $1/\beta$. This energy represents a characteristic upper limit and constitutes a necessary, though not sufficient, condition for cosmic-ray acceleration. Effects such as drift, diffusion, or advection may prevent particles from remaining within the acceleration zone.

From the Hillas energy, one can derive a minimum kinetic power requirement that the source must provide:

$$Q_k \gtrsim 10^{44} \text{ erg s}^{-1} \ \beta^{-1} \left(\frac{E/Z}{10^{19} \text{ eV}}\right)^2 \eta_B \ \eta^2, \quad (3)$$

where η_B is the ratio of magnetic to kinetic power, and η is an efficiency factor related to the Bohm diffusion regime [3].

Since achieving $\eta \approx 1$ is challenging in relativistic accelerators, equations (2) and (3) are considered to define the basic energetic requirements. We will consider $\eta = 1$ from now on.

III. A JET-OBJECT INTERACTION SCENARIO AND ITS CR MAXIMUM ENERGY

The specific nature of the object is not critical. It could be a cloud from the interstellar medium that moves into the jet without being destroyed beforehand, since at a certain height above the jet base, the cloud may appear as a very compact object; it could be a star producing a stellar wind that enters the jet (the wind creates an interaction region in which the ram pressures of the wind and the jet balance, forming a *bow shock*); it could be an AGB star undergoing intense mass loss over a relatively short period of time; it could be a supernova, corresponding to a mass ejection on the order of the stellar core's mass (this ejecta initially expands rapidly); etc. In any case, we assume that the interaction creates a *bow shock* region where particles can be accelerated.

Evolved stars or compact stellar systems typically cross an extragalactic jet on a timescale of $\sim r_j/v_{\text{obj}} \approx 10^6 \, r_{j,100\,\text{pc}} \, v_{\text{obj},7}^{-1}$ years, assuming a reference distance of $\lesssim 1$ kpc from the galactic plane [4]. We will assume that such objects, unless located very close to the jet base, evolve unaffected, as their supersonic winds prevent the jet from directly impacting them.

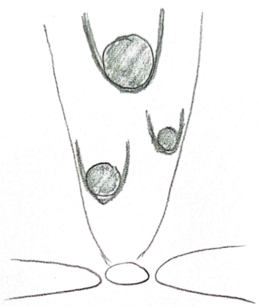

FIG. 1: Sketch of the simplified model.

A. Acceleration mechanism

To understand the mechanism of shock acceleration, let us imagine the jet as being composed of particles moving nearly at the speed of light in the direction of the jet. This flow impacts a denser obstacle made up of particles as well (such as atoms or, if the gas is hot and ionized enough, free protons and electrons). We can imagine this obstacle as a bubble made of balls with different velocities, but which, as a whole, expands with a certain characteristic velocity.

When the jet collides with the obstacle, a contact region is created between the two media that prevents significant mixing due to electromagnetic interactions. This region forms a contact discontinuity, from which two shocks emerge: one propagating back into the jet and another penetrating into the obstacle (see FIG. 1). These shocks decelerate the particles from the jet until, on average, they effectively come to rest. However, the energy of these particles is not lost—it is converted into thermal agitation (instead of ordered motion due to dynamics of the jet).

Inside the obstacle, particles that have gone through the shock are also compressed and heated, and the obstacle tend to expand sidewards. Shocks are essentially the propagation of compressed and hot material into the yet-unshocked material of the same object. The jet continues to push the shocked material, which therefore advances into the unshocked material. This process causes unshocked material to be incorporated into the shocked region, increasing its density and temperature. The particles in this compressed zone are closer together and move more chaotically.

The accelerated particles are some of these charged particles that, instead of colliding directly with one another, interact with the electromagnetic fields within the plasma (which are highly complex). Less energetic particles tend to move more erratically and cover shorter distances in a given time; more energetic ones can travel further. The Larmor radius gives us an idea of how a non-relativistic particle behaves in a magnetic field (it orbits around it). If the magnetic field is disordered (turbulent, chaotic, etc.), charged particles interact with these fields and are deflected. However, the more energetic the particle, the larger its Larmor radius, making it harder for the electromagnetic field to deflect it, allowing it to travel greater distances.

Thus, within the plasma, most particles have an average energy and a small Larmor radius, but a few more energetic ones can move more freely (they can propagate significantly through the plasma and explore regions with relativistic relative velocities). These particles can cross the boundary between the shocked and unshocked medium, back and forth, and gain energy with each cycle. We can picture this process as a ball bouncing between two walls that are moving closer together: each bounce gives it more energy. In reality, these "walls" are magnetic fields that deflect the particles and transfer energy to them.

Eventually, when the Larmor radius of a particle becomes as large as the size of the obstacle, it can escape the acceleration region. We assume that the maximum energy is reached when the gyroradius becomes comparable to the size of the obstacle. In that case, the escape time can be estimated as the obstacle size divided by the speed of light. We focus on the immediate shock region rather than particles escaping around the obstacle. To see more about diffusive shock acceleration, see e.g. [11].

B. Protons

For our exploration of the jet-object interaction scenario, we took $L_j = 10^{44}$ erg s^{-1} as the reference value for the jet power because significantly less powerful jets should not be able to accelerate UHECRs to the highest energies [6]. So the thresholds seen in the previous section are satisfied. On the other hand, significantly more powerful jets are very rare in the local Universe (see, e.g., [8]), and UHECRs cannot come from significantly beyond 100 Mpc (e.g., [9]; [10]). For the plots, we will study values between $L_j = 10^{43} - 10^{45}$ erg s^{-1}.

The jet-object interaction is assumed to occur around a region of the jet with radius $R_j = 0.1$ kpc, corresponding to the jet radius at the object's location. For a jet with a semi-opening angle $\theta \sim 0.1$ rad, the corresponding distance from the jet base (i.e., from the galactic nucleus to the object) is $z_j \sim 1$ kpc, given that $R_j \sim z_j \cdot \theta$. For the plots, we will study values between $z_j = 10^2 - 10^4$ pc. See FIG. 1 for all these considerations.

One can estimate the magnetic field from the electromagnetic component of the jet power. Let L_B denote the jet power (or luminosity) associated with its electromagnetic component—often referred to as the magnetic component, in a loose sense. L_B is often also known as the Poynting flux. We assume that the magnetic field power in the lab frame scales linearly with the total jet power, $L_B \propto L_j$, and introduce the parameter $\eta_B = L_B/L_j$ to quantify this relation. Adopting $L_B \sim L_j$ is likely too optimistic, a plausible range for the magnetic energy fraction is $0.01 \lesssim \eta_B \lesssim 1$.

The magnetic (or electromagnetic) component of the jet power is given by $L_B = \eta_B L_j$, where η_B is the fraction of the total jet power L_j carried by the magnetic field. Assuming a quasi-cylindrical, steady-state jet region with constant magnetic field B_j, the Poynting flux is given by $L_B = \pi R_j^2 v_j \frac{B_j^2}{4\pi}$, where R_j is the local radius of the jet, $v_j (\approx c)$ its velocity, and B_j the magnetic field at the location of the object (assumed constant in that region). Combining the two expressions above yields

$$B_j^2 = \frac{4\eta_B L_j}{R_j^2 v_j}. \quad (4)$$

This expression allows us to estimate the magnetic field strength in the jet as a function of the macroscopic jet parameters: $B_j = B_j(\eta_B, L_j, R_j, v_j)$. Accordingly, we will explore a range of plausible magnetic field strengths B_j at the relevant location in the jet.

This scenario defines an acceleration region (the shock region) where particles gain energy at a rate given by

$$\dot{E}_{\rm acc} = \eta_{\rm acc} q B_j \beta_j c. \tag{5}$$

Here, q is the elementary charge (or Zq for nuclei), which in CGS units has a value of 4.8×10^{-10} statC; $\eta_{\rm acc}$ is an efficiency parameter constrained within $0 \leq \eta_{\rm acc} \leq 1$; and $\dot{E}_{\rm acc}$ is the acceleration rate, i.e., the amount of energy gained by a particle per unit time. The acceleration time is given by $t_{\rm acc} = E/\dot{E}_{\rm acc}$, the duration over which the particle is subject to acceleration processes.

Particle acceleration occurs in the region where the jet shock takes place. We assume that acceleration takes place in the interaction region, which has a size comparable to that of the obstacle. Assuming no radiative losses, the shocked particles can be accelerated for at most the time they remain in this region. We suppose that the particles move along with the fluid surrounding the obstacle. The escape velocity of the particles in the acceleration region is nearly c. As they accelerate, their gyroradius increases. When they reach a gyroradius comparable to the size of the obstacle, they can cross it in a time of the order of R/c, and therefore this is the maximum acceleration time (residence time). The parameter $\eta_{\rm acc}$ gives us an idea of the fraction of the gyroradius from which a particle can escape or not. If $\eta_{\rm acc} = 1$, the size of the object $R_{\rm obj}$ will be equal to the gyroradius. If $\eta_{\rm acc} > 1$, a particle with a gyroradius smaller than $R_{\rm obj}$ may escape earlier.

Nuclei accelerated in the jet-ejecta interaction can reach an energy $E_{\rm max}$ and escape the region in a time before cooling or disintegrating via synchrotron, γ-meson production, $e^{\pm}$ creation, and photodisintegration (see, e.g., [1]; [3]); the cooling and disintegration times are $> 10^5$ yr. So, we neglect energy losses, or equivalently, we assume that the energy loss timescale is much longer than the acceleration timescale.

A particle within the interaction region requires a characteristic time to escape the body, given by $t_{\rm esc} = R_{\rm obj}/c$, where $R_{\rm obj}$ is the characteristic size of the object.

We assume $t_{\rm acc} = t_{\rm esc}$, meaning that the acceleration region (i.e., the shock region) coincides with the entire volume of the object. In this scenario, the time a particle takes to escape the object is equal to the time it takes to be accelerated (neglecting energy losses). Under this assumption, we obtain a maximum energy $E_{\rm max}$, representing an upper limit to the energy up to which protons (or nuclei) can be accelerated:

$$E_{max} = \eta_{acc} q B_j \beta_j R_{\rm obj} \tag{6}$$

Substituting the value of B_j, we obtain:

$$E_{max} = 2 q R_{\rm obj} \eta_{acc} \eta_B^{1/2} R_j^{-1} v_j^{1/2} c^{-1} L_j^{1/2} \tag{7}$$

By parametrizing the object radius inside the jet as $R_{\rm obj} = \eta_R R_j = \eta_R \cdot 0.1 \cdot z_j$, we obtain:

$$E_{max} = 2 q \eta_{acc} \eta_R \eta_B^{1/2} v_j^{1/2} c^{-1} L_j^{1/2} \tag{8}$$

so $E = E_{max}(\beta_j, \eta_{acc}, \eta_R, \eta_B, L_j)$. We consider different values for the parameters $\eta_{\rm acc} = 0.01 - 1$ and $\eta_R = 0.01 - 1$, in order to explore various acceleration efficiencies and object sizes. See the plots in FIG. 2.

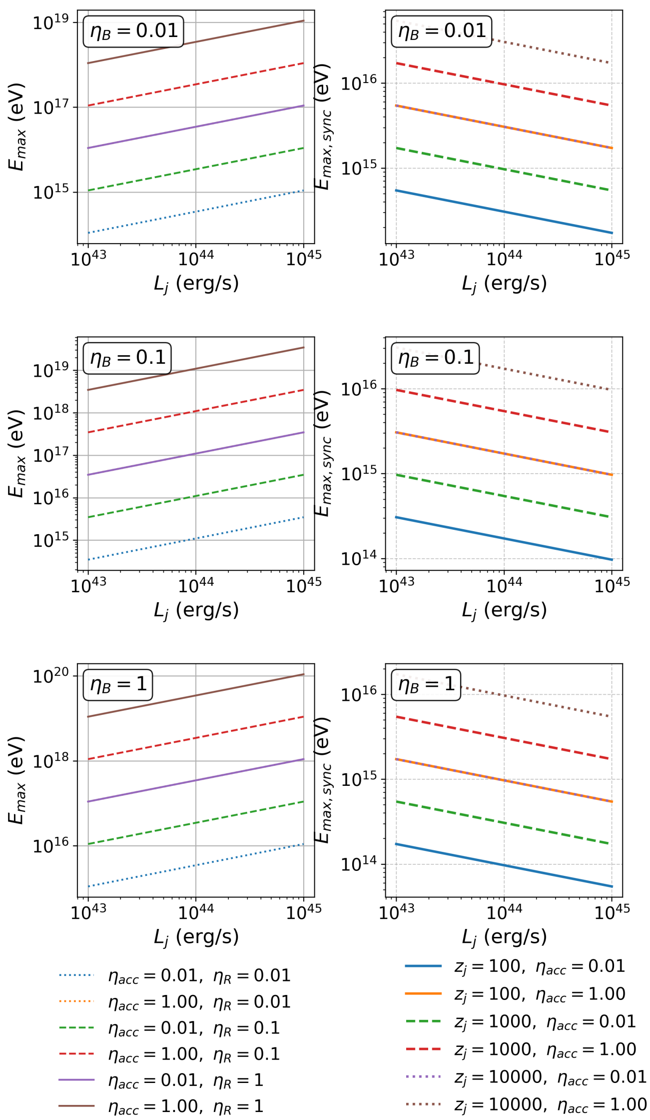

FIG. 2: Comparison of $E_{\rm max}$ versus L_j for different parameters. Left (subsection B, referring to protons): varying η_R, η_B, and $\eta_{\rm acc}$. Right (subsection C, referring to electrons): varying η_B, $\eta_{\rm acc}$, and z_j.

C. Electrons

The previously mentioned Hillas and power requirements, as well as the maximum energy derived from shock acceleration, apply in cases where the maximum cosmic ray (CR) energy is limited by the escape timescale. However, in sources with intense magnetic fields or strong radiation fields, energy losses may instead impose the dominant constraint on the maximum energy.

In our simplified model, we assume that synchrotron losses for protons and heavier nuclei are negligible compared to the acceleration timescale, and can therefore be safely ignored. This assumption is justified by the fact that the synchrotron energy loss rate scales as $\dot{E}_{\rm sync} \propto (m_e/m)^4$, where m_e is the electron mass and m is the mass of the radiating particle. For protons, this factor is approximately $(m_e/m_p)^4 \sim 10^{-13}$, making their synchrotron losses many orders of magnitude smaller than those of electrons, regardless of charge Z (see, e.g., [12]). However, for electrons, synchrotron cooling becomes a significant effect. The synchrotron cooling timescale for electrons is given by $\tau_{\rm sync}^{e^-} = 142\ {\rm yr} \cdot E_{\rm EeV}^{-1} B^{-2}$. Equivalently, the synchrotron energy loss rate can be approximated by

$$\dot{E}_{\rm sync} \approx -1.6 \times 10^{-3} B^2 E^2. \tag{9}$$

By equating the loss timescale with the acceleration timescale (see Eq. 5), we obtain an expression for the maximum energy achievable in a magnetic field of strength B:

$$E_{\rm max,sync} = \left(\frac{\eta_{\rm acc} q \beta_j c}{1.6 \times 10^{-3} B_j} \right)^{1/2} \tag{10}$$

Substituting the value of B_j, we obtain:

$$E_{\rm max,sync} = \left(\frac{\eta_{\rm acc} q \beta_j^{3/2} c^{3/2} z_j}{3.2 \times 10^{-2} \eta_B^{1/2}} \right)^{1/2} L_j^{-1/4}, \tag{11}$$

(see $E_{\rm max,sync} = E_{\rm max,sync}(\beta_j, \eta_{\rm acc}, z_j, \eta_B, L_j)$ in FIG. 2), so even under optimistic acceleration conditions, synchrotron losses can impose restrictive limits on the maximum achievable energy in sources with intense magnetic fields. Equivalently, one can invert the expression for the synchrotron-limited energy to derive an upper bound on the magnetic field strength for a given energy, highlighting the difficulty of accelerating electrons in highly magnetized environments.

IV. CONCLUSIONS

- This work presents a semi-analytical approach that provides both intuitive and quantitative insights into how the interaction between AGN jets and embedded objects can be a robust source of UHECRs. The model lays the groundwork for future extensions, such as numerical simulations or more detailed treatments of microphysics.
- A simple physical model has been constructed to describe such interaction. This model focuses on the formation of a bow shock region, where particles can be efficiently accelerated via diffusive shock acceleration. The mechanism satisfies the minimal physical conditions for acceleration.
- A general expression for the maximum energy ($E_{\rm max}$) attainable by a particle in the jet-object interaction scenario has been derived based on geometric and energetic considerations. The generated plots show the dependence of $E_{\rm max}$ on parameters such as L_j, z_j, η_R, η_B, and $\eta_{\rm acc}$, and indicate that, for reasonable values, energies close to 100 EeV can be achieved (see FIG. 2). The adopted parameter values are consistent with observations and recent literature.
- A complementary analysis for electrons has been included, showing that synchrotron cooling can severely limit their acceleration. In contrast, for protons and heavy nuclei, such losses are negligible in this context.

Acknowledgments: I would like to thank my supervisor, Valentí, for his guidance throughout the work.

[1] Hillas, A.M.. "The Origin of Ultra-High-Energy Cosmic Rays". Ann. Rev. Astron. Astrophys. (1984).
[2] Rieger, F.M.. "Active Galactic Nuclei as Potential Sources of Ultra-High Energy Cosmic Rays". (2022). arXiv:2211.12202 [astro-ph.HE].
[3] Matthews, J.H. and Taylor, A.M.. "How, where and when do cosmic rays reach ultrahigh energies?" Proc. Sci., PoS(ICRC2021) **394** (2023). arXiv:2301.02682 [astro-ph.HE].
[4] V. Bosch-Ramon, "The role of supernovae inside AGN jets in UHECR acceleration", *Astronomy & Astrophysics* **677**, L14 (2023). https://doi.org/10.1051/0004-6361/202347554
[5] J. Linsley, "Evidence for a Primary Cosmic-Ray Particle with Energy 10^{20}eV", Phys. Rev. Lett. (1963).
[6] M. Lemoine, "Extragalactic magnetic fields and the second knee in the cosmic-ray spectrum", Nucl. Phys. B Proc. Suppl. **190**: 174 (2009).
[7] A. Aab, P. Abreu, M. Aglietta, et al., "Depth of maximum of air-shower profiles at the Pierre Auger Observatory: Measurements at energies above $10^{17.8}$ eV", Phys. Rev. D **90**: 122006 (2014).
[8] Mingo, B., Croston, J.H., Hardcastle, M.J., et al. "The population of radio galaxies at z ¡ 0.8 in the LOFAR Twometre Sky Survey (LoTSS) DR1". *Mon. Not. R. Astron. Soc.* **488**, 2701 (2019).
[9] Greisen, K. "End to the Cosmic-Ray Spectrum?" *Phys. Rev. Lett.* **16**, 748 (1966).
[10] Zatsepin, G.T. and Kuz'min, V.A. "Upper Limit of the Spectrum of Cosmic Rays". *Sov. J. Exp. Theor. Phys. Lett.* **4**, 78 (1966).
[11] L. O'C. Drury, "An introduction to the theory of diffusive shock acceleration of energetic particles in tenuous plasmas", *Rep. Prog. Phys.* **46**, 973–1027 (1983).
[12] Rybicki, G.B. and Lightman, A.P., *Radiative Processes in Astrophysics*. Wiley-VCH, 1986.

Acceleració de raigs còsmics d'energia ultraalta mitjançant interaccions entre jets i obstacles en jets extragalàctics de nuclis galàctics actius

Author: Pol Quingles Daví
Facultat de Física, Universitat de Barcelona, Diagonal 645, 08028 Barcelona, Spain.

Advisor: Valentí Bosch, vbosch@fqa.ub.edu

Resum: Els jets dels nuclis galàctics actius són potencials acceleradors de raigs còsmics d'energia ultraalta (UHECRs). Alguns objectes poden romandre en la regió del jet durant períodes prolongats i contribuir a l'acceleració de raigs còsmics, especialment de nuclis pesants. Hem explorat el paper de les interaccions entre jets i objectes dins de jets extragalàctics en la producció de UHECRs. El nostre objectiu ha estat caracteritzar les energies màximes de les partícules accelerades en aquests esdeveniments, probablement dominats per nuclis pesants, i avaluar si aquestes interaccions poden actuar com a llocs d'acceleració. Hem trobat que les interaccions jet-objecte poden generar acceleradors prou eficients, produint raigs còsmics amb energies de fins a 100 EeV. Aquestes interaccions poden contribuir significativament a la població de raigs còsmics mitjançant l'acceleració directa de partícules.
Keywords: galàxies: actives – galàxies: nuclis – galàxies: jets – raigs còsmics
SDGs: ODSs 4 i 7

Objectius de Desenvolupament Sostenible (ODSs o SDGs)

1. Fi de les desigualtats		10. Reducció de les desigualtats	
2. Fam zero		11. Ciutats i comunitats sostenibles	
3. Salut i benestar		12. Consum i producció responsables	
4. Educació de qualitat	X	13. Acció climàtica	
5. Igualtat de gènere		14. Vida submarina	
6. Aigua neta i sanejament		15. Vida terrestre	
7. Energia neta i sostenible	X	16. Pau, justícia i institucions sòlides	
8. Treball digne i creixement econòmic		17. Aliança pels objectius	
9. Indústria, innovació, infraestructures			